SUPPLEMENTARY INFORMATION

Plasticity tunable artificial synapses based on organic electrochemical transistors with aqueous electrolyte

Ruhua Wu[a], Miao Xie [a], Yuhua Cheng[a], Dan Zhao*[a], Liang-Wen Feng *[b], Jianhua Chen *[c], and Wei Huang*[a]

[a] School of Automation Engineering, University of Electronic Science and Technology of China (UESTC), Chengdu 611700, China.

[b] Key Laboratory of Green Chemistry& Technology, Ministry of Education, College of Chemistry, Sichuan University, Chengdu 610065, China

[c] Department of Chemical Science and Technology, Yunnan University, Kunming 650091, China

Supplementary Figures

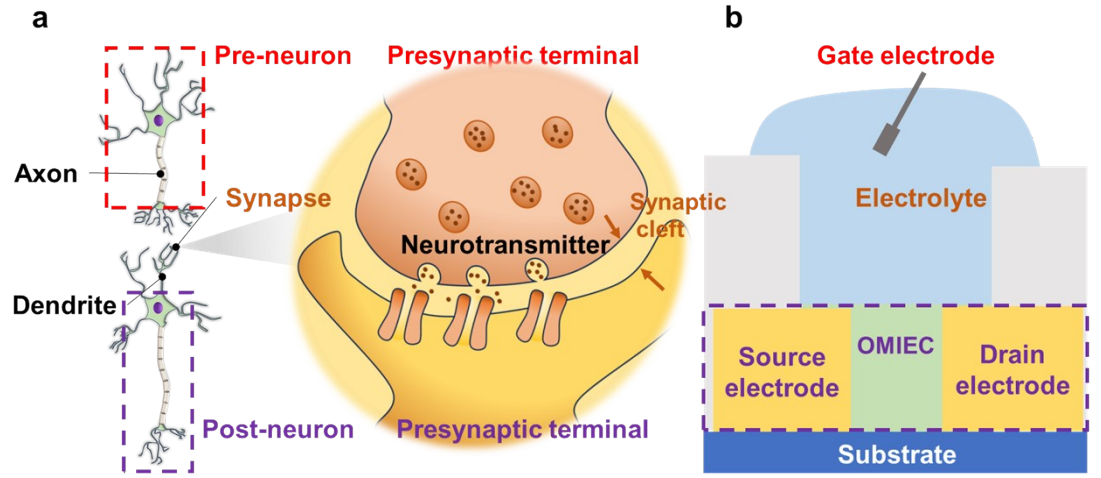

Figure S1. Schematic of (a) a biological synapse and (b) a synaptic OECT, where the OMIEC channel and the source/drain electrodes mimic the postsynaptic terminal of a biological synapse, while the aqueous electrolyte (PBS 1×) and the Ag/AgCl gate electrode mimic the synaptic cleft and presynaptic terminal, respectively.

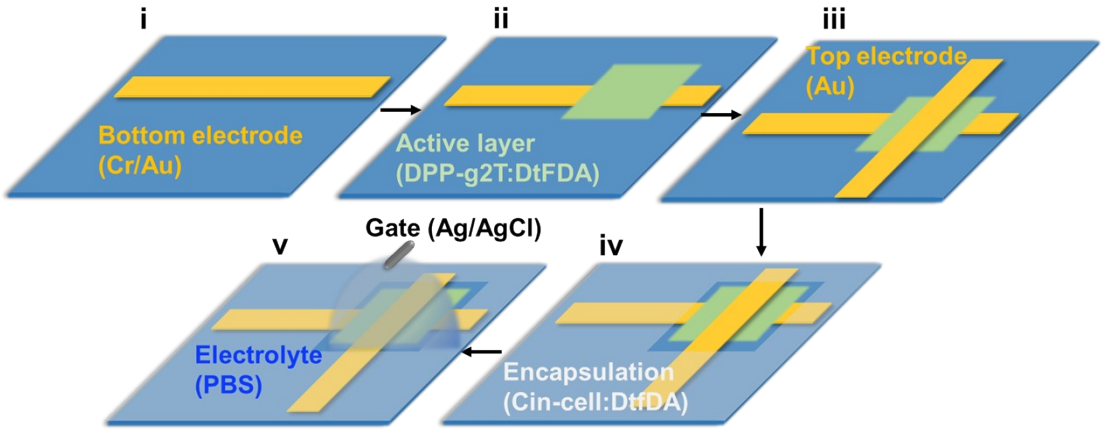

Figure S2. Fabrication process of the synaptic vOECT. i) Bottom electrode evaporation. ii) Active channel layer spin-coating and patterning. iii) Top electrode evaporation. iv) Encapsulation layer spin-coating and patterning. v) PBS electrolyte application and Ag/AgCl gate electrode insertion.

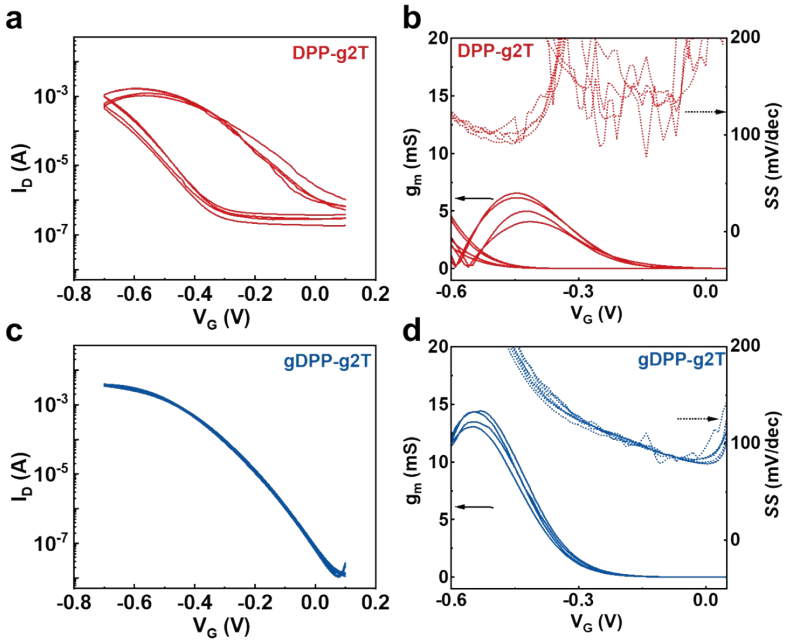

Figure S3. (a,c) Transfer characteristics and (b,d) g_m/SS characteristics of 4 individual vOECTs based on (a,b)DPP-g2T and (c,d) gDPP-g2T. $W_B = W_T = 60$ μm, $V_D = -0.1$ V.

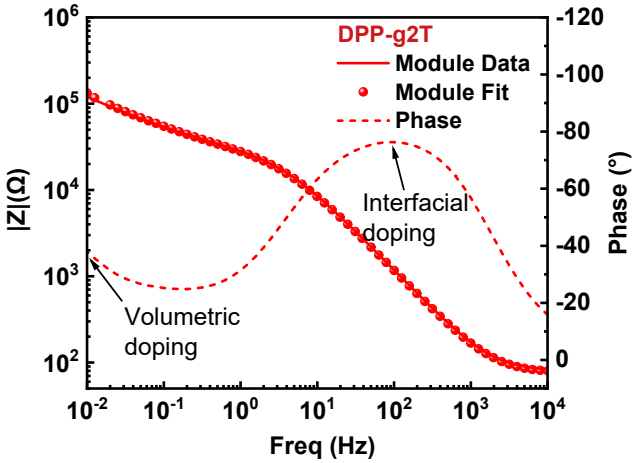

Figure S4. EIS curve of DPP-g2T polymer thin film with a frequency range from 0.01 to 10000 Hz.

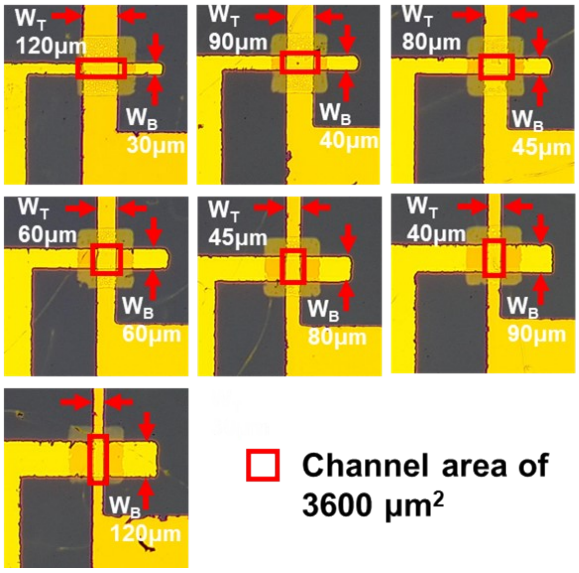

Figure S5. Microscopic photos of vOECTs with varied widths of top and bottom electrodes, where the channel area is maintained at 3600 μm^2 for all devices.

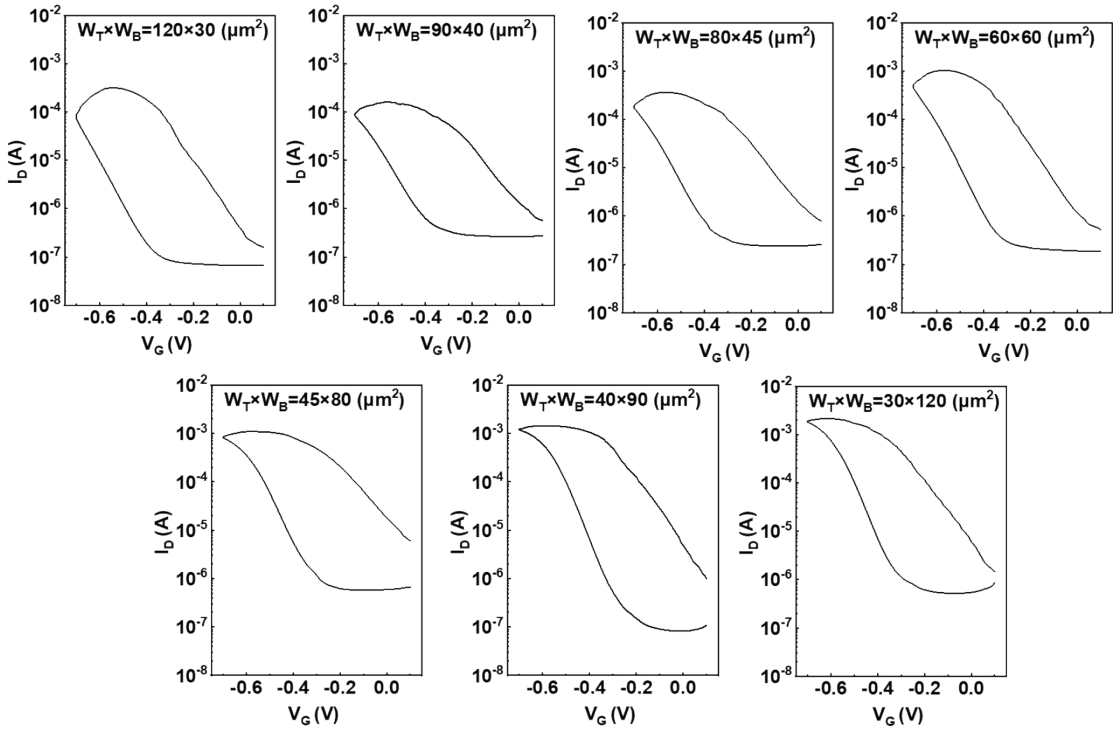

Figure S6. Transfer curves of the devices with different channel dimensions, including $W_T \times W_B$ of 120×30 μm^2, 90×40 μm^2, 80×45 μm^2, 60×60 μm^2, 45×80 μm^2, 40×90 μm^2, 30×120 μm^2, respectively. V_D=-0.1 V.

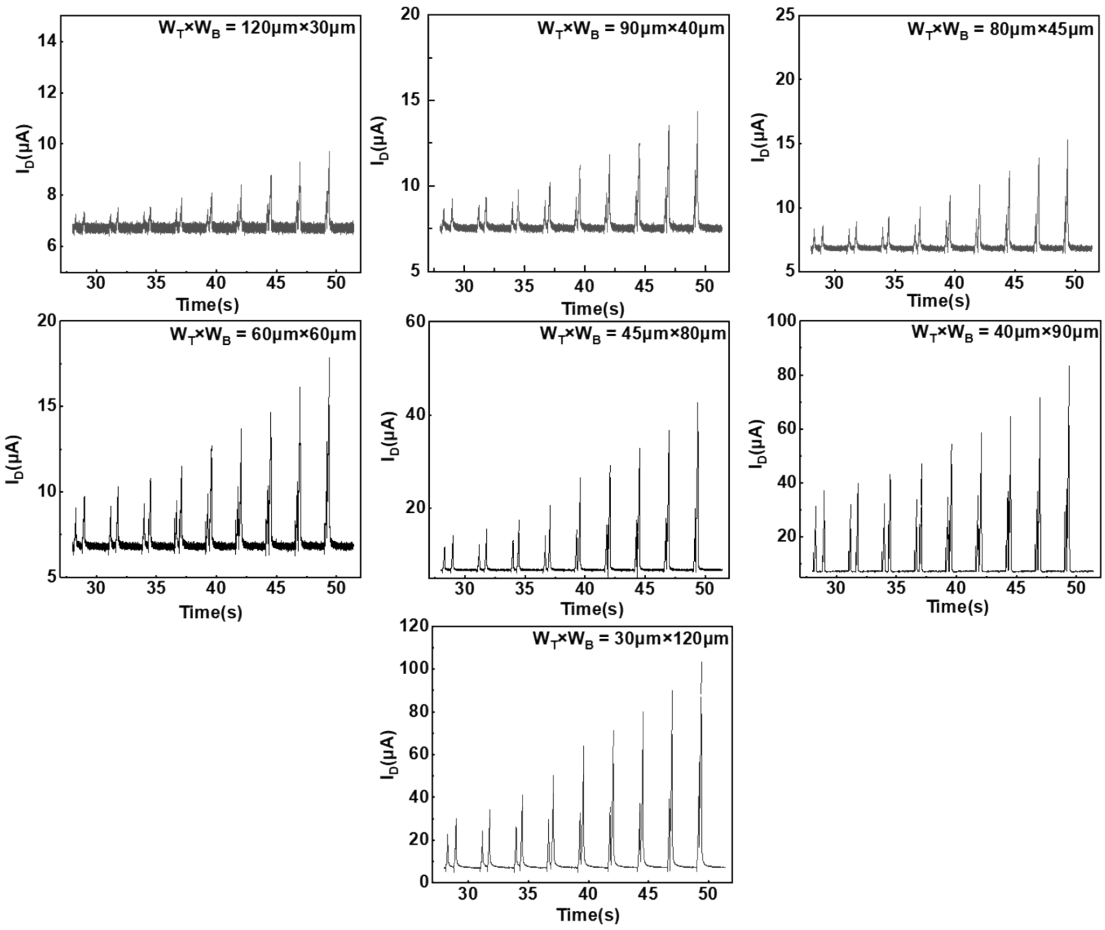

Figure S7. Plots of paired-pulse facilitation with different electrode dimensions by applying couples of pulses (500 ms, -0.7 V) with varied intervals (20 ms to 1 s).

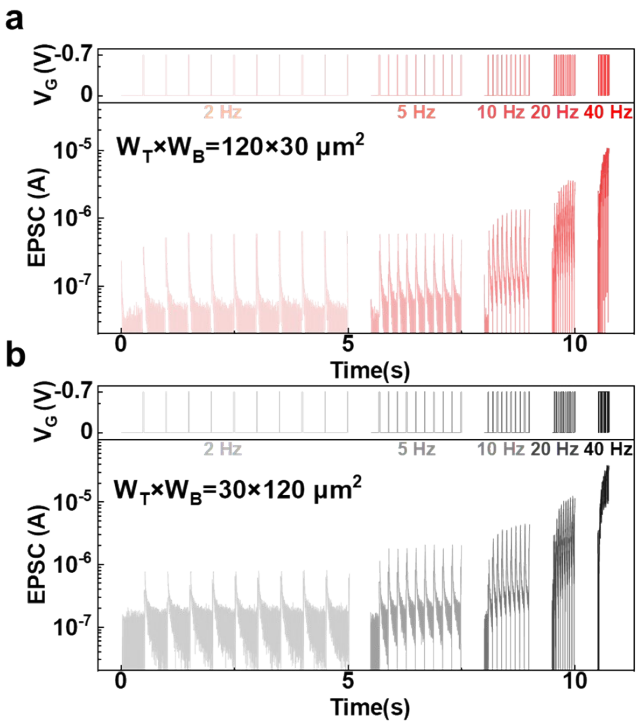

Figure S8. Dynamic filtering by recording EPSC response under input bias (-0.7 V, 20 ms) with different frequencies applied for vOECTs with $W_T \times W_B$ of (a) 120×30 μm^2 and (b) 30×120 μm^2.

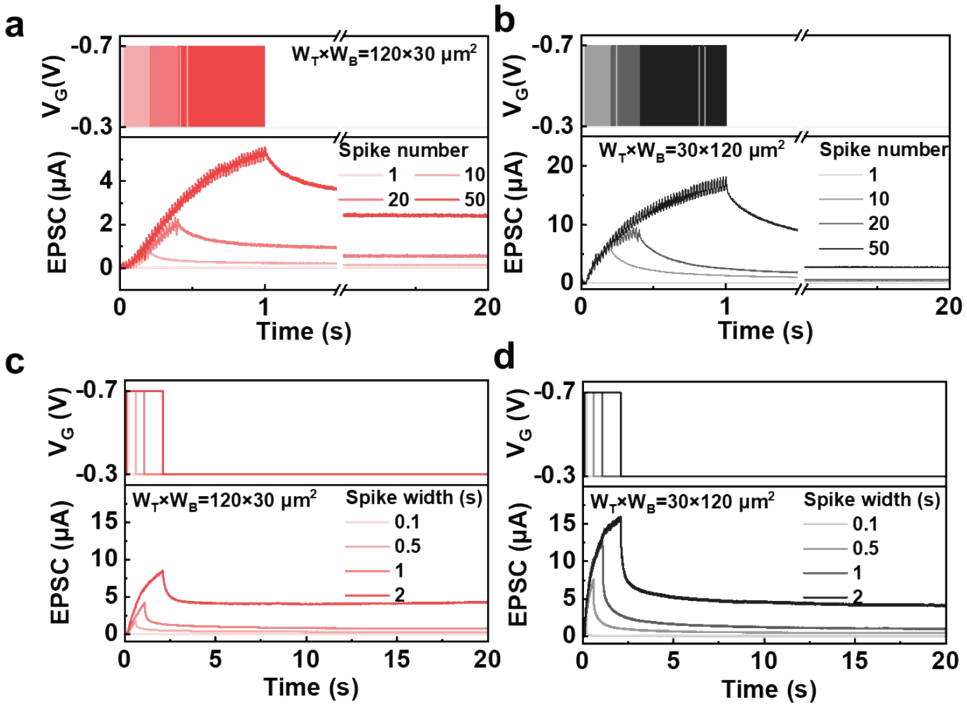

Figure S9. Plots of SNDP and the presynaptic bias of the vOECT with $W_T \times W_B$ of (a) 120×30 μm^2 and (b) 30×120 μm^2 and the SDDP of the vOECT with $W_T \times W_B$ of (c) 120×30 μm^2 and (d) 30×120 μm^2

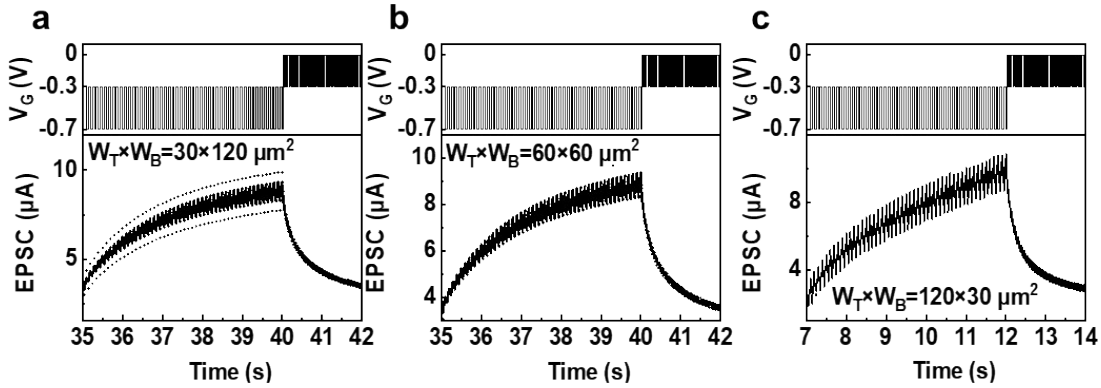

Figure S10. 100 states of the LTPo and LTD EPSC responses with varied electrode dimensions.

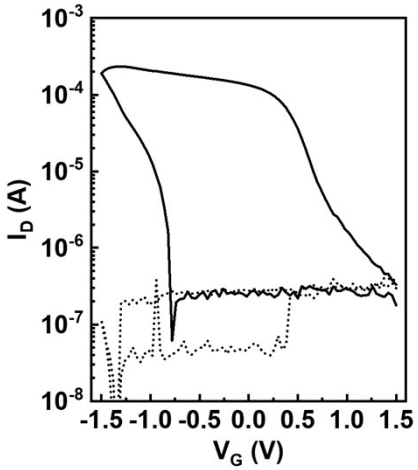

Figure S11. Transfer characteristic of vOECT synapse with DPP-g2T functionalized Au side gate.

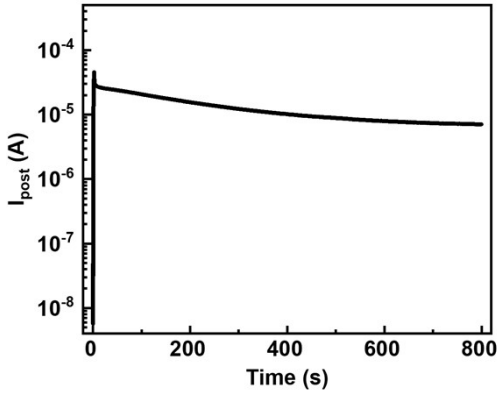

Figure S12. Long-term state retention for 800 s of a DPP-g2T gated vOECT synapse after a presynaptic stimulus with a spike width of 2 s and amplitude of 1.2 V.